Similar coherence between heavy-hole and light-hole excitons has been reported in (*33*). These are examples of quantum coherence involving a nonradiative superposition of states, which leads to many novel phenomena such as the Hanle effect, dark states, lasing without inversion, electromagnetically induced transparency, and population trapping [see (*33*) and references therein]. However, unlike the QD system, atomic Zeeman coherence does not necessarily involve two differentiable electrons, in contrast to the experiment we present here.

Finally, it is critical to note that while the simple discussion related to Fig. 1 shows the origin of the entanglement, the discussion is considerably over-simplified; it completely disregards the possibility that fast dephasing of the Zeeman coherence could lead to an unobservable effect, even if the single-exciton states themselves were long-lived. In the language of NMR, this is saying that a long T_1 and T_2 associated with the single-exciton states does not guarantee a comparable T_2 for the Zeeman coherence. The magnitude of the decoherence rate, γ_{ij} $(1/T_2)$, in Eq. 2 can be determined by comparing the relative strength of the coherent and incoherent contribution. The dephasing rate of the radiative coherence was already shown in (*24*) to be ~20 ps and is comparable to the energy relaxation rate, Γ $(1/T_1)$. This measurement further gives the decay rate of the Zeeman coherence as ~20 ps, which again is similar to the energy relaxation rate and shows that the pure dephasing of the two-exciton coherence is not significant in QDs. By exchanging the spectral position of the pump and the probe (the polarization has to be changed accordingly, too), the relative time scale of incoherent spin relaxation can also be estimated. As expected, the Zeeman splitting has reduced this process to an unobservable level (>100 ps).

In summary, we have inferred from our measurements entanglement of an excitonic system in single GaAs QDs and shown the importance of exciton-exciton Coulomb interaction for this observation. Our results are explained by a three-level model in a two-exciton basis. The next step, though more challenging, is to recover the same type of entanglement between coupled QDs [as proposed, for example, in (*13, 14*)]. This would allow for scaling the experiment to larger systems.

References and Notes

1. A. Einstein, B. Podolsky, N. Rosen, *Phys. Rev.* **47**, 777 (1935).
2. E. Schrödinger, *Proc. Camb. Philos. Soc.* **31**, 555 (1935).
3. R. J. C. Spreeuw, *Found. Phys.* **28**, 361 (1998).
4. For an introductory review, see the special issue on quantum information [*Phys. World* **11**, 33 (March 1998)].
5. See the review by A. Zeilinger [*Rev. Mod. Phys.* **71**, S288 (1999)] for discussions on entangling photons.
6. C. A. Sackett *et al.*, *Nature* **404**, 256 (2000).
7. Q. A. Turchette *et al.*, *Phys. Rev. Lett.* **81**, 3631 (1998).
8. E. Hagley *et al.*, *Phys. Rev. Lett.* **79**, 1 (1997).
9. See the article in the Search and Discovery section [*Phys. Today* **53**, 20 (January 2000)] for discussions on entanglement in liquid-state NMR. For experimental demonstrations of quantum algorithms using NMR, see, for example, I. L. Chuang *et al.*, *Phys. Rev. Lett.* **80**, 3408 (1998).
10. C. Monroe, D. M. Meekhof, B. E. King, W. M. Itano, D. J. Wineland, *Phys. Rev. Lett.* **75**, 4714 (1995).
11. Q. A. Turchette, C. J. Hood, W. Lange, H. Mabuchi, H. J. Kimble, *Phys. Rev. Lett.* **75**, 4710 (1995).
12. J. Ahn, T. C. Weinacht, P. H. Bucksbaum, *Science* **287**, 463 (2000).
13. A. Ekert and R. Jozsa, *Rev. Mod. Phys.* **68**, 733 (1996).
14. D. Loss and D. P. DiVincenzo, *Phys. Rev. A* **57**, 120 (1998).
15. A. Imamoglu *et al.*, *Phys. Rev. Lett.* **83**, 4204 (1999).
16. G. Schedelbeck, W. Wegscheider, M. Bichler, G. Abstreiter, *Science* **277**, 1792 (1997).
17. C. B. Murray, C. R. Kagan, M. G. Bawendi, *Science* **270**, 1335 (1995).
18. L. J. Sham and T. M. Rice, *Phys. Rev.* **144**, 708 (1966).
19. For two noninteracting systems under the excitation scheme described in the text, the total wavefunction is factorizable. This is explicit from the total Hamiltonian of the system, which is a sum of two independent Hamiltonians describing each system under excitation. The coupling needed for entanglement is provided through a number of ways under different circumstances. In cavity QED, the atoms are coupled through cavity fields. The Coulomb interaction provides the coupling for entangling two trapped ions and in our case, two excitonic transitions in a single quantum dot.
20. T. Östreich, K. Schönhammer, L. J. Sham, *Phys. Rev. Lett.* **75**, 2554 (1995).
21. See, for example, K. Bottet *et al.*, *Phys. Rev. B* **48**, 17418 (1993).
22. K. Brunner, G. Abstreiter, G. Böhn, G. Tränkle, G. Weimann, *Phys. Rev. Lett.* **73**, 1138 (1994).
23. In the case of entangling two trapped ions (*7*), one needs to rely on their common phonon modes that result from the Coulomb interaction. Since the ions are well separated in space, the weak interaction only creates collective motional modes without affecting their internal states. Therefore, none of the electronic states within one ion is mixed with those of its neighbor. Each level of the four-level model would in fact consist of a series of sublevels with the phonon modes incorporated. For some carefully arranged excitation (red-sideband excitation) and a specific initial condition (two-ion ground state with one phonon), no sublevels in the fourth (upper-most) level are resonant with the laser beams, resulting in a zero-probability amplitude of this level and therefore a nonfactorizable wavefunction.
24. N. H. Bonadeo *et al.*, *Phys. Rev. Lett.* **81**, 2759 (1998).
25. For our experiment, the pump and probe fields (E_{pump} and E_{probe}) are amplitude-modulated by two standing-wave acousto-optical modulators at frequency f_{pump} and f_{probe}, respectively. These frequencies (~100 MHz) are sufficient to suppress the slow nonelfectronic nonlinearities as well as the Overhauser effect present in the system. The third-order coherent nonlinear field $E^{(3)}_{\text{NL}}$ proportional to $\chi^{(3)}$ $E_{\text{pump}}E^{*}_{\text{pump}}E_{\text{probe}}$ is emitted along the probe direction. A photodetector placed in the transmitted probe beam along with a lock-in amplifier phase-locked to $f_{\text{pump}} - f_{\text{probe}}$ detects signal that is proportional to the real part of $E^{(3)}_{\text{NL}}E^{*}_{\text{probe}}$ [the imaginary part of $\chi^{(3)}$]. The pump and the probe are from the same laser for the degenerate experiment and from two separate but mutually coherent lasers for the nondegenerate experiment.
26. D. Gammon, E. S. Snow, B. V. Shanabrook, D. S. Katzer, D. Park, *Phys. Rev. Lett.* **76**, 3005 (1996).
27. ______, *Science* **273**, 87 (1996).
28. S. W. Brown, T. A. Kennedy, D. Gammon, *Phys. Rev. B* **54**, R17339 (1996).
29. I. M. Beterov and V. P. Chebotaev, *Prog. Quantum Electron.* **3**, 1 (1974).
30. The mutual coherence bandwidth for the two lasers must be less than the decay rate of the coherence between the two excitons. The two lasers used in our measurement have a mutual bandwidth of about 3 MHz.
31. C. Sieh *et al.*, *Phys. Rev. Lett.* 82, 3112 (1999).
32. C. H. Bennett, D. P. DiVincenzo, J. A. Smolin, W. K. Wootters, *Phys. Rev. A* **54**, 3824 (1996).
33. K. Ferrio and D. Steel, *Phys. Rev. Lett.* **80**, 786 (1998).
34. This work was supported in part by the National Security Agency and Advanced Research and Development Activity under Army Research Office grant DAAG55-98-1-0373, Air Force Office of Scientific Research grant F49620-99-1-0045, NSF grant DMR 97-21444, and the Office of Naval Research. We thank R. Merlin, P. Berman, H. J. Kimble, D. Wineland, and D. DiVincenzo for helpful discussions, and R. Merlin for loaning critical equipment.

29 March 2000; accepted 4 August 2000

Evidence That the Reactivity of the Martian Soil Is Due to Superoxide Ions

A. S. Yen,[1]* S. S. Kim,[1] M. H. Hecht,[1] M. S. Frant,[2] B. Murray[3]

The Viking Landers were unable to detect evidence of life on Mars but, instead, found a chemically reactive soil capable of decomposing organic molecules. This reactivity was attributed to the presence of one or more as-yet-unidentified inorganic superoxides or peroxides in the martian soil. Using electron paramagnetic resonance spectroscopy, we show that superoxide radical ions (O_2^-) form directly on Mars-analog mineral surfaces exposed to ultraviolet radiation under a simulated martian atmosphere. These oxygen radicals can explain the reactive nature of the soil and the apparent absence of organic material at the martian surface.

The 1976 Mars Viking Landers performed a series of experiments in which soil samples were analyzed for evidence of life. Biological responses were not detected; however, the soil samples from the surface as well as from ~10 cm beneath the immediate surface were found to be chemically reactive (*1*). Upon the introduction of water vapor, oxygen was released from the soil samples in larger quantities than would be expected from physical adsorption in equilibrium with the ambient atmosphere (*2*). Furthermore, isotopically labeled organic nutrient solutions were decomposed when exposed to the soil (*3*). It was also discovered that the surface was devoid of organic molecules above part-per-billion levels (*4*), including molecules that are likely delivered by meteoric infall (*5*). These results are consistent with a hypothesis that there is one or more reactive oxidants present at the martian surface (*6*). However, none of the candidates described in the existing literature (*7*) provide a complete explanation for the soil reactivity.

[1]Jet Propulsion Laboratory, California Institute of Technology, 4800 Oak Grove Drive, Pasadena, CA 91109, USA. [2]Chemotics Consulting, 131 Westchester Road, Newton, MA 02458, USA. [3]California Institute of Technology, Division of Geological and Planetary Sciences, 1200 East California Boulevard, Pasadena, CA 91125, USA.

*To whom correspondence should be addressed. E-mail: Albert.Yen@jpl.nasa.gov

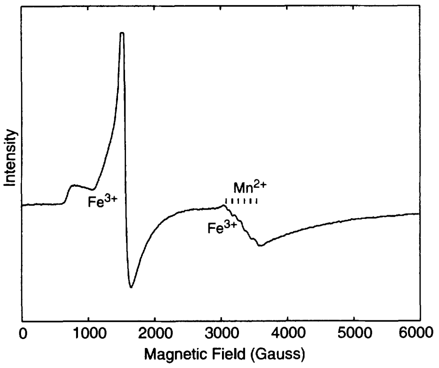

Fig. 1. Intensity versus field strength for a wide range X-band (~9 GHz) EPR scan of plagioclase feldspar, a likely component of the martian regolith. The signal contains broad iron as well as manganese features. The values on the vertical axis in this and subsequent plots are in arbitrary units because the scale is dependent on the choice of receiver gain factor.

Here, we propose that superoxide radical ions (O_2^-) are responsible for the chemical reactivity of the martian soil. We demonstrate in the laboratory a process for the formation of O_2^- on Mars on the basis of known environmental elements, including ultraviolet (UV) photons, atmospheric oxygen, mineral grain surfaces, and extremely low concentrations of water vapor. The formation of reactive oxygen species, such as O^-, O_2^-, and O_3^-, on material surfaces under similar conditions has been well established in the laboratory (*8–10*). The UV photons mobilize electrons, which are subsequently trapped at the surface and are readily captured by oxygen molecules, thus forming surface adsorbates (*11*).

We extend the applicability of this process to Mars by investigating the formation of oxygen radicals on natural mineral surfaces under Mars-like atmospheric conditions and radiation environment. Our experiments were based on electron paramagnetic resonance (EPR) detection and identification because of its high sensitivity to species with unpaired electrons (*12*). We selected labradorite, a plagioclase feldspar, as the mineral substrate in our experiments (*13*) because of its abundance in basalts and its presence in reconstructions of Mars Global Surveyor thermal emission spectrometer data (*14*).

A broad EPR scan (over 6000 Gauss) of the plagioclase feldspar under 6 mbar of a Mars gas mixture is dominated by iron and manganese impurities (Fig. 1). A narrow scan (over 40 Gauss) of the same sample before and after a 20-hour exposure to a low-pressure mercury vapor lamp (peak flux at 254 nm) shows a UV radiation-induced change (Fig. 2). This feature is located at the g = 2 region (*12*) of the spectrum, confirming the production of radical species. The sample was placed on a cold plate maintained at –30°C during exposure, and the UV photons were transmitted through a portion of the tube not used for the EPR analyses (*15*).

Three samples of plagioclase feldspar were pumped down to 10^{-6} torr, backfilled with different partial pressures of oxygen (10 mtorr, 1 torr, and 700 torr), and then exposed to UV radiation for 5 hours. The lowest concentration represents the approximate partial pressure of oxygen on Mars. Larger signal intensities resulted from samples with greater concentrations of oxygen, indicating that the radical species are derived from oxygen (*16*). Thermal tests show that the oxygen radical signature survived heating to 200°C (Fig. 3). These results are consistent with adsorbed superoxide anions (O_2^-) forming on the feldspar grains: O_2^- is known to be stable at temperatures in excess of 300°C, whereas the other common oxygen radicals, O^- and O_3^-, do not survive beyond 100°C (*17*). The shape and g values (2.0046 for the primary resonance) of the features in our spectra are also consistent with O_2^-.

Our experiments demonstrate UV-induced production and retention of superoxide ions on Mars-analog mineral surfaces under a simulated martian atmosphere at and above ambient temperatures of the martian surface. The key elements in this formation process are all present on Mars: UV radiation, mineral surfaces, atmospheric oxygen, and extremely low concentrations of water vapor. We expect O_2^- to form and to be stable in the absence of reactants at the martian surface. In contrast, many of the suggested oxidants, such as hydrogen peroxide (*18*), will decompose either in the presence of transition metal oxides or exposure to the daytime UV radiation flux (*7*). The plagioclase feldspar samples used in the laboratory experiments exhibit the characteristic EPR signals from Fe^{3+} and Mn^{2+}, yet the O_2^- remains on the grain surfaces. Of the radical species most commonly formed by UV exposure in the presence of oxygen (O^-, O_2^-, and O_3^-), O_2^- is the least reactive and hence the most stable. It is also the most likely oxygen radical species to be present in the range of temperatures (~140 to 300 K) (*19*) at the martian surface (*11*). Our

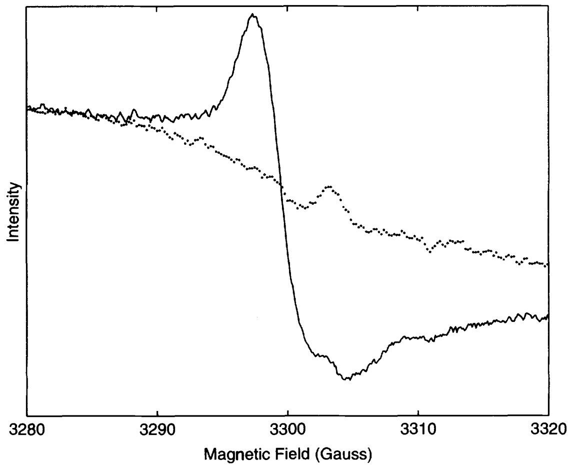

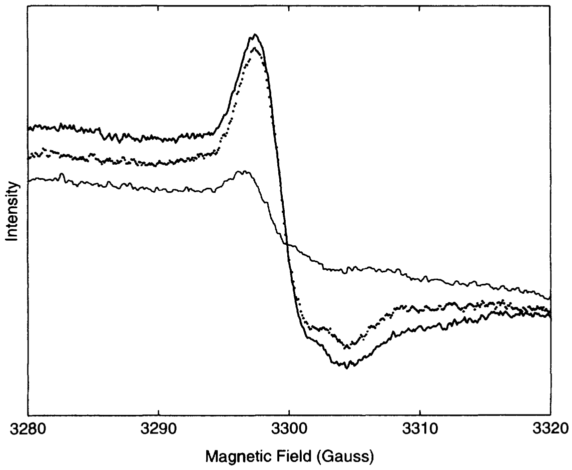

Fig. 2 (left). Detailed EPR scan over a 40-Gauss range of the sample scanned in Fig. 1 before (dotted line) and after (solid line) treatment by UV photons for 20 hours under a simulated martian atmosphere. The signature of adsorbed oxygen radicals is evident after irradiation. **Fig. 3 (right).** A feldspar sample with adsorbed oxygen radicals produced by exposure to UV radiation (thick line), after heating to 100°C for 1 hour (dotted line), and after an additional heating cycle to 200°C for 1 hour (thin line). The signal intensity is reduced by 10% at 100°C, but 30% of the original signal remains after the second heat treatment at 200°C.

experiments show little or no degradation of the signal in samples maintained at room temperature for over 1 week. Furthermore, the temperature stability of this species (Fig. 3) is consistent with results from the Viking gas exchange experiment where soil reactivity persisted after heating to 145°C under a He purge for 3.5 hours (*2, 20*).

The Viking experiments found that soil samples collected from underneath a rock and from about 10 cm beneath the surface exhibited reactive characteristics similar to soil at the immediate surface. Photogenerated oxygen radicals must, therefore, be mobile to provide an adequate explanation of the spacecraft data. Experimental studies clearly show that O_2^- molecules undergo two-dimensional diffusion across material surfaces (*21*). Hops between adsorption sites on SiO_2 substrates occur on time scales of 2×10^{-8} s to 2.6×10^{-9} s at −196°C and 25°C, respectively (*22, 23*). This mobility of O_2^- varies with the composition of the substrate (*24*), but the range of measured and calculated repositioning times is between 10^{-9} and 10^{-3} s (*25*). These values are short relative to geologic time scales and are consistent with diffusion over the cm-scale distances necessary to explain the reactivity of subsurface soils (*26*).

The reactivity of oxygen ions has been investigated extensively, and experimental data show that alkanes, alkenes, aromatics, and other hydrocarbons are efficiently oxidized by O_2^- adsorbed on surfaces (*27, 28*). In the presence of water, the superoxide ion reacts to produce oxygen, the perhydroxyl radical, and the hydroxyl radical (*29*)

$$2O_2^- + H_2O \rightarrow O_2 + HO_2^- + OH^-$$

The release of oxygen during the humidification and injection of water into martian soil by the Viking Landers can be explained by this reaction. The decomposition of organic nutrients in the Viking experiments is consistent with the production of HO_2^- and OH^- species after the aqueous solutions were introduced. The absence of organic molecules, including those delivered by meteoric infall, at the martian surface is likely due to decomposition by oxygen radicals and/or by the products of O_2^- reactions with atmospheric water vapor.

Analyses at the Viking 1 landing site showed that a 1-cm^3 soil sample produced 690 nM of oxygen after 50 hours at 100% relative humidity (*30*). On the basis of the reaction described above, a bulk density of 1.3 g/cm^3 (*30*) and an estimated surface area of 17 m^2/g (*31*), we estimate an abundance of 4×10^{12} superoxide ions per cm^2 of soil surface area on Mars. Using laboratory calibrations with the free radical DPPH (1,1-diphenyl-2-picrylhydrazyl) and a measured surface area from gas adsorption of 4.2 m^2/g for our feldspar samples, we estimate that we produced $\sim 8 \times 10^9$ O_2^- ions per cm^2 of mineral surface area under a simulated martian atmosphere in a 20-hour exposure. This irradiation time, which is geologically short, does not allow adequate time for ion diffusion through the sample, so a more appropriate comparison is between the abundance per cm^2 of soil surface on Mars to what is produced in the lab per cm^2 of cross section exposed to the UV lamp (~2 cm^2). Using 2 cm^2 as the appropriate area, we calculate a production of 10^{13} O_2^- ions per cm^2 of surface, which is consistent with the abundance of 4×10^{12} ions/cm^2 estimated for Mars.

In the laboratory, we produced a total of 3×10^{13} O_2^- ions in the 100-mg feldspar sample after 20 hours of exposure. Most of these superoxide radicals, however, were generated in the first hour of exposure with an easily measurable signal (10^{13} spins) after only 30 min under the UV lamp. We estimate the initial formation rate in the experiments to be at least 10^9 O_2^- radicals per second, which corresponds to a quantum yield of $\sim 10^{-6}$ radicals per photon (*32*).

An approximate integral of the solar UV model presented in (*33*) indicates that $\sim 10^{13}$ photons between 2000 Å and 3500 Å interact with each cm^2 of martian surface per second during daylight hours (*34*). This incident power is a factor of $\sim 10^2$ lower than in our experiments and suggests that O_2^- radicals can form at a rate of 10^7 per cm^2 of cross-sectional area each second at the martian surface. The 4×10^{12} superoxide ions per cm^2 of soil surface area on Mars inferred from the Viking Lander results could form in less than 2 weeks if all the grain surfaces were exposed to the incident photons. Thus, the formation time is rapid. This process may be limited by the rate of exposure of surfaces not previously populated with O_2^-, either by overturning of the soil or by diffusive transport of superoxide ions to greater depths in the regolith (*35*).

On the basis of our experiments under simulated martian conditions, we expect adsorbed superoxide radicals (O_2^-) to form readily on mineral grains at the surface of Mars. The stability, mobility, and reactivity of O_2^- are all consistent with the Viking Lander results, and we believe that the presence of these oxygen radicals is the most straightforward explanation for the unusual reactivity of the martian soil and for the apparent absence of organic molecules.

References and Notes

1. H. P. Klein *et al.*, *Science* **194**, 99 (1976).
2. V. I. Oyama and B. J. Berdahl, *J. Geophys. Res.* **82**, 4669 (1977).
3. G. V. Levin and P. A. Straat, *J. Geophys. Res.* **82**, 4663 (1977).
4. K. Biemann *et al.*, *J. Geophys. Res.* **82**, 4641 (1977).
5. S. F. S. Chun, K. D. Pang, J. A. Cutts, J. M. Ajello, *Nature* **274**, 875 (1978).
6. H. P. Klein, *Icarus* **34**, 666 (1977).
7. A. P. Zent and C. P. McKay, *Icarus* **108**, 146 (1994).
8. M. Che and A. J. Tench, *Adv. Catal.* **31**, 77, (1982).
9. ———, *Adv. Catal.* **32**, 1, (1983).
10. J. H. Lunsford, *Catal. Rev.* **8**, 135, (1973).
11. T. Ito *et al.*, *J. Chem. Soc., Faraday Trans.* **81**, 2835 (1985).
12. EPR spectroscopy is based on measuring transitions between spin states of unpaired electrons by varying the applied magnetic field while irradiating the sample at microwave frequencies (*36*). When the magnetic field reaches the point at which the energy difference between the two allowed orientations of the electron spin is equal to the microwave quantum ($h\nu$), a detectable resonance occurs. Atoms and molecules with unpaired electrons are identified by their characteristic resonance spectra, as well as the "g value," defined by $g = h\nu/\beta H$ where h is Planck's constant, ν is the microwave frequency (in our case X-band, ~9 GHz), β is the Bohr magneton, and H is the applied magnetic field. The g value of a free electron is 2.0023, and thus, radical species such as O_2^- have a signature near the $g = 2$ region of the spectrum. All EPR data for this study were collected at liquid nitrogen temperature to ensure the retention of metastable species created by the UV radiation.
13. Labradorite samples from Ponderosa Mine, Oregon (*37*) have a low concentration of paramagnetic cations, which minimizes interference with the characterization of the reactive adsorbates. To increase the surface area available for adsorption, we crushed and sieved the samples to retain particles less than 75 micrometers in size. Samples (100 mg) were placed inside 4-mm diameter supracil EPR tubes, vacuum dried to minimize adsorbed water, and sealed under a simulated martian atmosphere. The gas mixture was obtained from Matheson Gas Products (Rancho Cueamonga, CA) and was certified to contain 2.7% N_2, 1.6% Ar, and 0.2% O_2 in a CO_2 carrier.
14. Spectra of the bright martian soils obtained from the thermal emission spectrometer were reconstructed with a mixture consisting of 12% labradorite (*38*). In addition, recent analyses suggest that low albedo regions of Mars contain greater than 35% feldspar with the dominant phase being plagioclase (*39*).
15. During exposure to the ultraviolet photons, the powdered sample was shifted to the upper one-third of the ~20-cm tube. The remaining two-thirds of the tube was shielded from the lamp. The shielded, lower portion of the tube was used for EPR analyses of the sample so that radiation damage to the tube would not appear as a false signal.
16. Web fig. 1 is available at *Science* Online at www.sciencemag.org/feature/data/1051956.shl.
17. M. Anpo *et al.*, *J. Phys. Chem.* **89**, 5689 (1985). See also (*11*).
18. D. M. Hunten, *J. Mol. Evol.* **14**, 71, 1979.
19. H. H. Kieffer *et al.*, *J. Geophys. Res.* **82**, 4249 (1977).
20. The Viking labeled release experiment found that heating of a soil sample to 46°C substantially reduced the ability to decompose the nutrient solution and that heating to 160°C for 3 hours completely eliminated the reactivity. These findings are in contrast with the thermal stability results of the gas exchange experiment but do not necessarily require the presence of two chemically distinct oxidants (one thermally stable and the other, labile). The difference could be due to experimental procedures (*40*). The labeled release experiment heated the samples in a closed chamber, and water vapor released from the soil (*4*) could have destroyed the reactive species. The samples in the gas exchange experiment, on the other hand, were heated in the presence of a purge gas, which would have removed water vapor from the chamber. This interpretation is supported by an anomalous gas exchange heating experiment where the failure of a drain valve prevented the exhaust of chamber gases and resulted in an unreactive sample (*2*).
21. R. B. Clarkson and R. G. Kooser, *Surf. Sci.*, **74**, 325 (1978).
22. Translation of O_2^- across a surface is coupled with reorientation of the radical, and the shape of the EPR spectra depends on the orientation. Thus, EPR data are used to determine the time scales associated with mobility on various substrates (*25*).
23. R. F. Howe and W. C. Timmer, *J. Chem. Phys.* **85**, 6129 (1986).

24. R. F. Howe, *Colloids and Surf. A: Physicochem. Eng. Aspects* **72**, 353 (1993).
25. ———, *Adv. Colloid Interface Sci.* **18**, 1 (1982).
26. An application of published activation energies (*24*) to diffusion time scales in the martian soil is inappropriate because there is limited information on the effects of grain boundaries on the mobility of the O_2^- radicals. We believe that migration of surface-generated O_2^- across soil grains to a depth of 10 cm or more is certainly possible on geologic time scales, but more work is necessary to characterize the mobility of this species in a granular material.
27. J. H. Lunsford, *Am. Chem. Soc. Sympos. Ser.* **248**, 127 (1984).
28. A. M. Gasymov *et al.*, *Kinet. Katal.* **25**, 358 (1984).
29. F. A. Cotton, G. Wilkinson, P. L. Gaus, *Basic Inorganic Chemistry* (Wiley, New York, 1995), pp. 435–443.
30. V. I. Oyama, B. J. Berdahl, G. C. Carle, *Nature* **265**, 110 (1977).
31. E. B. Ballou, P. C. Wood, T. Wydeven, M. E. Lehwalt, R. E. Mack, *Nature* **271**, 644 (1978).
32. The UV lamp used in the experiments has an output of 10^{-3} W/cm^2. The ~2 cm^2 of sample cross section exposed to the lamp corresponds to a capture of ~10^{15} photons per s at a wavelength of 254 nm.
33. W. R. Kuhn and S. K. Atreya, *J. Mol. Evol.* **14**, 57 (1979).
34. The long wavelength cutoff for photons capable of generating oxygen radicals on martian mineral grains is inherently uncertain because the band gap for mobilizing electrons depends on the specific content of impurities. However, the use of 3500 Å for this order-of-magnitude estimate is reasonable.
35. The concentration of oxygen in the martian troposphere (~0.13% by volume) is high enough to allow more than 10^{18} collisions with each cm^2 of soil surface area each second. This value is at least 10 orders of magnitude greater than the total number of oxygen radicals we expect to form on Mars in 1 s; therefore, we conclude that the oxygen abundance is not a limiting factor.
36. D. L Perry, *Instrumental Surface Analysis of Geologic Materials* (VCH, New York, 1990).
37. C. L. Johnston, M. E. Gunter, C. R. Knowles, *Gems and Gemology* **27**, 220 (1991).
38. P. R. Christensen *et al.*, *Science* **279**, 1692 (1998).
39. J. L. Bandfield, V. E. Hamilton, P. R Christensen, *Science* **287**, 1626 (2000).
40. N. H. Horowitz, *To Utopia and Back: The Search for Life in the Solar System* (Freeman, New York, 1986), p. 136.
41. This work was performed at the Jet Propulsion Laboratory, California Institute of Technology, under contract to the National Aeronautics and Space Administration.

5 May 2000; accepted 2 August 2000

Osmium Isotopic Evidence for Mesozoic Removal of Lithospheric Mantle Beneath the Sierra Nevada, California

Cin-Ty Lee[1]*, Qingzhu Yin,[1] Roberta L. Rudnick,[1]†
John T. Chesley,[2] Stein B. Jacobsen[1]

Thermobarometric and Os isotopic data for peridotite xenoliths from late Miocene and younger lavas in the Sierra Nevada reveal that the lithospheric mantle is vertically stratified: the shallowest portions (<45 to 60 kilometers) are cold (670° to 740°C) and show evidence for heating and yield Proterozoic Os model ages, whereas the deeper portions (45 to 100 kilometers) yield Phanerozoic Os model ages and show evidence for extensive cooling from temperatures >1100°C to 750°C. Because a variety of isotopic evidence suggests that the Sierran batholith formed on preexisting Proterozoic lithosphere, most of the original lithospheric mantle appears to have been removed before the late Miocene, leaving only a sliver of ancient mantle beneath the crust.

Lithospheric removal, in the form of detachment, foundering, or peeling away of the lithospheric mantle with or without lower crust into the convecting mantle, has been predicted by various geodynamic models (*1–4*) and may have important geochemical implications (*5*, *6*). For lack of a better term, these forms of lithospheric removal are referred to here as "delamination" in order to distinguish them from lithospheric removal associated with extension or upwelling-induced erosion (*7*). Finding direct evidence for delamination is difficult: although delamination is predicted to cause increased magmatism, changes in magmatic composition, high elevations, high rates of uplift, and low P_n velocities (*8–12*), these phenomena can also be explained by extension or active upwelling.

The extinct Mesozoic Sierra Nevada arc is one place where removal of the underlying subcontinental lithospheric mantle (SCLM) has been proposed. The Sierra Nevada is characterized by high elevations, low P_n velocities (*9–11*), and variable xenolith assemblages (*12*). The latter have been interpreted to reflect delamination of an eclogitic lower crust (*12*). Because the Sierra Nevada was built on Proterozoic lithosphere, as evidenced by radiogenic Sr and ~1.6 Ga Sm-Nd model ages in batholithic rocks (*13*, *14*), the present Sierran SCLM should be young if delamination occurred during or after arc formation. However, many Cenozoic basalts [18 million years ago (Ma) to the present] erupted throughout the Sierra Nevada and western edge of the Great Basin have high $^{87}Sr/^{86}Sr$, low $^{143}Nd/^{144}Nd$, and low $^{3}He/^{4}He$ ratios, which collectively have been interpreted to derive from ancient [>0.8 billion years ago (Ga)] lithospheric mantle (*15–17*). Here, we use Os isotopes and major-element partitioning between mineral phases (thermobarometry) in lithospheric mantle xenoliths to determine the age of the SCLM and to estimate their pressure and temperature conditions, thereby allowing us to evaluate the extent and nature of SCLM removal.

The Re-Os isotopic system is the most robust method of dating the formation of SCLM (*18–21*), which is stabilized by conductive cooling and partial melting in the uppermost mantle. The latter produces a buoyant, refractory residue, having a low Re/Os ratio (Re is incompatible and Os is compatible in the residue during partial melting), which correlates with other indicators of fertility such as Ca and Al. Such a residue, if isolated in the SCLM, will develop low time-integrated $^{187}Os/^{188}Os$ relative to the convecting mantle. Ideally, one can use the Re/Os ratio of a peridotite along with its $^{187}Os/^{188}Os$ ratio to determine a Re-Os model age by extrapolating back to the point in time to where the peridotite's $^{187}Os/^{188}Os$ ratio intersects the mantle evolution curve (*21*). However, a number of factors may lead to Re/Os ratios that are not truly representative of the residual peridotite (*22*). In these cases, there are two other ways of determining model ages. "Re depletion" model ages (T_{RD}) assume that Re/Os is zero, and therefore yield minimum ages. For the most refractory peridotites, T_{RD} ages approximate the time of the melting event. Alternatively, major elements such as Ca and Al can be used as proxies for Re/Os, with the age of the melting event inferred from the $^{187}Os/^{188}Os$ intercept at Al_2O_3 = 0 (*23*). The Mg# [Mg/(Mg + Fe)] may also be used as an inverse proxy (*23*).

The large contrast between the age of the original Sierran lithosphere (~1.6 Ga) and the age of its hypothetical removal (Mesozoic and younger) is within the resolution of the

---

[1]Department of Earth and Planetary Sciences, Harvard University, 20 Oxford Street, Cambridge, MA 02138, USA. [2]Department of Geological Sciences, Gould-Simpson Building, Building 77, University of Arizona, Tucson, AZ 85712, USA.

*To whom correspondence should be addressed. E-mail: ctlee@eps.harvard.edu

†Present address: Department of Geology, University of Maryland, College Park, MD 20742, USA.